Materials Physics and Mechanics 42 (2019) 415-422 Received: April 16, 2018

# THE INFLUENCE OF STRESS TRIAXIALITY ON DUCTILITY OF α TITANIUM ALLOY IN A WIDE RANGE OF STRAIN RATES

**V.V. Skripnyak, A.A Kozulyn, V.A. Skripnyak***

National Research Tomsk State University, Russia

*e-mail: skrp2012@yandex.ru

**Abstract.** This work aimed to evaluate the combined effect of stress triaxiality and strain rate on the tensile behavior of the titanium alloy. The results of experimental studies and numerical modelling of the mechanical behavior of alpha titanium alloys were received and summarized. This paper presents the results of the research of mechanical behavior of titanium alloy VT 5-1 (this is an analog of Ti-5Al-2,25Sn) in a wide range of strain rates (from 0.001 to 1000 1/s) and stress triaxiality (0.0–0.6). Specimens of four different shapes were used in experiments to study the deformation and fracture under uniaxial tension, shear. Experimental studies were performed on servo-hydraulic test machine Instron VHS 40/50-20. The model of inelastic deformation and ductile damage criterion were proposed to describe the ductility of the titanium alloy in a wide range of strain rates and stress triaxiality.
**Keywords:** experiment, numerical modelling, alpha titanium alloys

## 1. Introduction

The study on the influence of the strain rate and its changes on the mechanical properties of alloys with high specific strength characteristics at strain rates from 1 to $10^3$ 1/s has important fundamental and applied value. The results of these studies are the basis for the creation of new, adequate models for predicting deformation, accumulation of structural damage and fracture of structural alloys under dynamic loading conditions [1,2,3,4]. The need for such models is due to the need to predict the durability and strength of structures using computer-aided engineering analysis of designed or operated structures from light alloys [5,6,7,8]. There is growing interest in titanium-based alloys [1,2,6,9,10,11]. Recent studies have shown that the strength properties of coarse-grained and ultrafine-grained titanium alloys change significantly with increasing strain rate [9,12,13]. Studies on the dynamics of the spall fracture of titanium alloys showed that the strength characteristics of alloys are higher with increasing concentration of the beta phase, and decreasing the average grain size [2,4]. It was found that a complex stress state significantly affects the strength characteristics of the titanium alloy Ti-6Al-4V [14].

There is evidence that the fracture of the hexagonal close-packed polycrystalline metals and alloys is strongly dependent on the accumulated plastic strain, represented by the equivalent plastic strain, and hydrostatic pressure. The hydrostatic pressure is represented by the dimensionless stress triaxiality factor $\eta=p/\sigma_{eq}$, defined as the ratio between the hydrostatic stress p and equivalent stress $\sigma_{eq}$. A significant distinction has been noted between the regimes of high and low-stress triaxiality. High values of triaxiality (i.e., $\eta > 1.5$) may be achieved in local areas, such as at the ends of the cracks or in the center of necking or notched specimen under tension. Low-stress triaxiality takes place at surfaces and protruding corners, where the equivalent shear stress is high relative to the hydrostatic pressure. At low-stress triaxiality, the fracture initiation is strongly inhibited. Several models were proposed to investigate the effect

http://dx.doi.org/10.18720/MPM.4242019_6

of the triaxiality on the fracture of polycrystalline metals and alloys [15,16]. Neilsen and Tvergaard [17] showed that ductile fracture can be described using the criterion, depending on the stress triaxiality and the Lode angle. Valoppi and others [14] used the phenomenological Johnson Cook hardening model and damage initiation criterion with an energy-based law describing the damage evolution in the FE models for titanium alloy. It was shown the Gurson–Tvergaard–Needleman plasticity model can be complemented with phenomenological laws for void nucleation, growth, and coalescence [5,18]. In this research, we study the influence of different stress triaxiality ($0.0< \eta < 0.6$) on ductile fracture in a wide range of strain rates using experimental tests and numerical simulation. Four types of VT 5-1 (Ti-5Al-2,25Sn) sheet samples were used in experiments on static and dynamic tension. Under the studied conditions of the tension of specimens in VT5-1 alloy, a macroscopic crack is formed as a result of nucleation and growth of damage at a lower structural level. In the framework of the mechanics of damaged media approach, ductile fracture of materials is considered as a result of the nucleation and growth of damage at the mesoscopic structural levelm for example, the voids.

## 2. Damage model

The GTN model [5,18] was used for analysis of stresses and strains in smooth and notched samples of sheet VT 5-1 under tension. The yield criterion has a form:

$$(\sigma_{eq}{}^2/\sigma_s{}^2)+2q_1f^*\cosh(-q_2\,p/2\sigma_s)-1-q_3(f^*)^2=0, \quad (1)$$

where $\sigma_s$ is the yield stress, $p$ is the pressure, $q_1$, $q_2$ and $q_3$ are model parameters, and $f$ is the void volume fraction.

The rate of void growth is obtained by assuming mass conservation and depends on the volume change part of the plastic strain.

Consequently, there is no void growth in pure shear deformation. The void nucleation depends on the equivalent plastic strain $\varepsilon_p$, here a normal distribution A is used:

A strong coupling between deformation and damage is introduced by a plastic potential function which is dependent on the void volume fraction $f^*$

$$\dot{f}=\dot{f}_{nucl}+\dot{f}_{growth},$$
$$\dot{f}_{nucl}=(f_N/s_N)\dot{\varepsilon}^p\exp\{-0.5[(\varepsilon^p{}_{eq}-\varepsilon_N)/s_N]^2\}, \quad (2)$$
$$\dot{f}_{growth}=(1-f)\dot{\varepsilon}^p_{kk},$$

where $\varepsilon_N$ and $s_N$ are the average nucleation strain and the standard deviation respectively. The amount of nucleating voids is controlled by the parameter $f_N$.

$$f^*=f \text{ if } f\le f_c;$$
$$f^*=f_c+(\bar{f}_F-f_c)/(f_F-f_c) \text{ if } f>f_c, \quad (3)$$

where $\bar{f}_F=(q_1+\sqrt{q_1{}^2-q_3})/q_3$, $q_1$, $q_2$ and $q_3$ are constants of the model.

The final stage in ductile fracture comprises of the voids coalescence into the fracture zone. This causes softening of the material and accelerated growth of the void fraction $f^*$ until the fracture void fraction $f_F$ is reached. At this moment the material is fractured. The model of ductile fracture requires knowledge of 9 parameters: three model parameters ($q_1$, $q_2$ and $q_3$), the initial void fraction $f_0$, three void nucleation parameters ($\varepsilon_N$, $s_N$, and $f_N$), two failure parameters ($f_c$ and $f_F$). The model parameters for titanium alloy VT 5-1 were

determined by numerical simulation of experiments on the tensile samples in the velocity range from 20 to 0.4 m/s. The numerical values of model parameters are given in Table 2. The model was used for simulation of titanium samples under tension at a constant velocity from 20 m/s to 0.4 m/s.

Table 1. Dimensionless parameters of the GTN model for the VT 5-1 (Ti-5Al-2,25Sn) sheets

| Parameter | $q_1$ | $q_2$ | $q_3$ | $f_0$ | $f_N$ | $f_c$ | $f_F$ | $\varepsilon_N$ | $s_N$ |
|---|---|---|---|---|---|---|---|---|---|
| Sheet of VT 5-1 | 1 | 0.7 | 1 | 0.003 | 0.1156 | 0.117 | 0.260 | 0.05 | 0.005 |

LS-DYNA solver integrated into WB ANSYS 14.5 software was used for finite element (FE) simulation of deformation and fracture processes.

## 3. Material and samples

The investigated material is VT 5-1 (Ti-5Al-2,25Sn) alpha titanium alloy. The thickness of the sheets samples was 1.15±0.05 mm. The sheet of VT 5-1 alloy does not have exactly the same chemical composition no the same microstructure. Table 1 shows the chemical composition of VT 5-1. VT 5-1 consists of a majority of the hexagonal close-packed alpha-phase.

Table 2. Chemical composition (weight percent) of VT 5-1 (Ti-5Al-2,25Sn) sheets

| Alloy | Fe | V | Al | Sn | Zr | C | O | N | Ti |
|---|---|---|---|---|---|---|---|---|---|
| VT 5-1 | 0.3 | 1.2 | 6.27 | 2.2 | 0.3 | 0.009 | 0.15 | 0.05 | balance |

The tensile tests were performed on samples characterized by different geometries, as shown in Fig. 1(a), in order to vary both the stress triaxiality and Lode parameter.
The stress triaxiality η and Lode parameters *L* defined as:

$$\eta = -p/\sigma_{eq},\ L = \left(2\sigma_{II} - \sigma_I - \sigma_{III}\right)/\left(\sigma_I - \sigma_{III}\right), \quad (4)$$

where p is the pressure, $\sigma_I$, $\sigma_{II}$, $\sigma_{III}$ are first, second, and third invariants of the Cauchy stress tensor respectively, $\sigma_{eq} = (3\sigma_{II})^{1/2}$ is the equivalent stress.

The stress triaxiality during the deformation is not constant. The initial triaxiality was calculated in the undeformed state by formula [19]:

$$\eta = (1+2D)/(3\sqrt{D^2+D+1}),\ D = \ln[1+a/(4R)], \quad (5)$$

where a is the width of a sample, *R* is the value of notch radius.

The samples were cut using the electro erosion cutting method from a sheet of titanium alloy with a thickness of ~1.18 mm. The thickness of samples was 1.18+0.01 mm, the initial sample length $l_0$ was equal to 24±0.1 mm, the cross-sectional area of the smooth flat samples was $A_0$=9.3±0.05 mm$^2$, notch flat specimens had notch radius of $R_1$=10 mm, $R_2$ = 5 mm, $R_3$=2 mm. The samples for the shear test had distance between cuts δ ~4.5 mm.

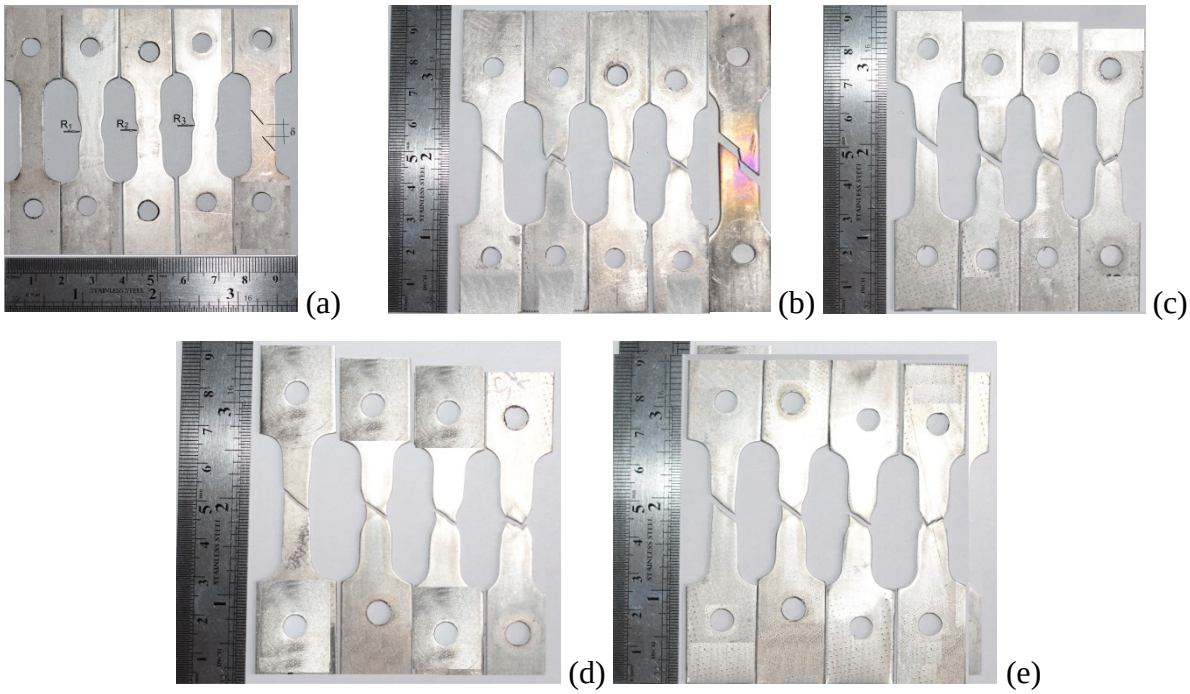


**Fig. 1.** (a) Geometry of the samples used for tensile and shear tests: $l_0$ =24±0.1 mm, $A_0$=9.3±0.05 mm$^2$, notch radius: $R_1$=10 mm, $R_2$ = 5 mm, $R_3$=2 mm, distance between cuts δ =4.5 mm. (b) Fractured samples after tension at the velocity: 20 m/s , (c) 12 m/s, (d) 2.4 m/s, (e) 0.4 m/s

## 4. Quasistatic and dynamic tests

The tests were carried within the range of strain rates (16−833 s$^{-1}$) at room temperature using an Instron test machine VHS 40/50-20 with a 50 kN load cell. The tests were conducted at constant tensile velocity 20±0.01, 12±0.01, 2.4±0.002, 0.4±0.001 m/s. Tests were divided into three groups: (I) uniaxial tensile tests carried out on smooth specimens, characterized by positive values of both the stress triaxiality and the Lode parameter. The second group is pure shear tests. The third group is uniaxial tensile tests carried out on flat notch specimens. Two values of notch radius, 2 mm, and 10 mm, were used in this study. The true strain and the true stress were determined using the analytical formulas:

$$\varepsilon_1^{true} = \ln(1+\Delta l / l_0),\ \sigma_1^{true} = (F / A_0)(1+\Delta l / l_0), \quad (6)$$

where $\varepsilon_1^{true}$ is true strain, $\sigma_1^{true}$ is true stress, $F$ is tensile force, $A_0$ is mean initial minimum cross sectional area of sheet sample, $\Delta l$ is the change in gauge length, $l_0$ is the initial gauge length.

## 5. Results

Photos of fractured samples after tension are showed in Fig. 1(b). The true flow stress versus true strain at room temperature and strain rate 834 s$^{-1}$ (at the velocity 20 m/s) are shown in Fig. 2(a). Measured values of strain to fracture at strain rates 833±5, 418 ±2, 100±1, 16.7±1 s$^{-1}$ of smooth and notch samples are shown in Fig. 2(b).

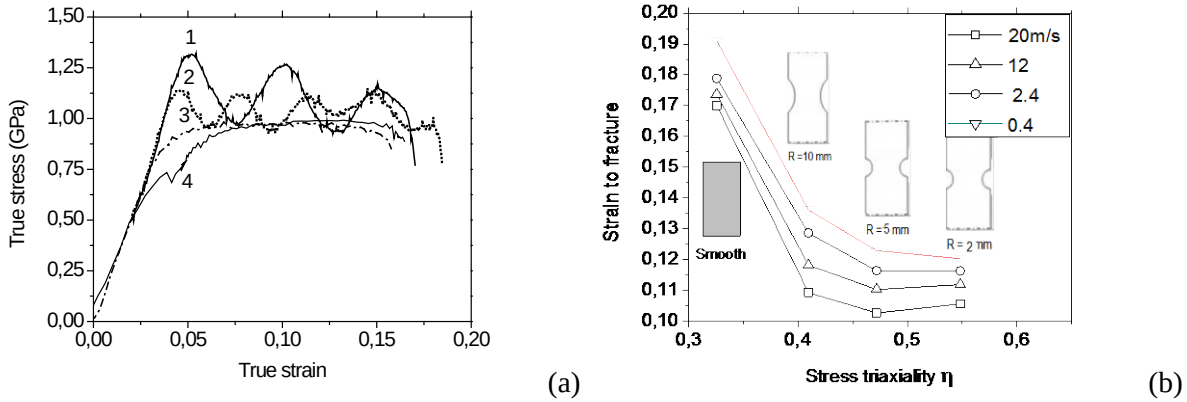


(a) (b)

**Fig. 2.** (a) True flow stress versus true strain for smooth samples (η=0.33) at room temperature. Curves 1-4 correspond to velocities of tension: 20±0.01, 12±0.01, 2.4±0.002, 0.4±0.001 m/s respectively. (b) Strain to fracture of titanium VT 5-1 samples under axial tension at velocities 20, 12, 2.4, 0.4 m/s and at the initial stress triaxiality η: 0.3333, 0.4087, 0.4681, and 0.5491

Calculated effective plastic strains, effective stresses, and tensile strength in the notched sample with R=10 mm are shown in Fig. 3. The velocity of tension is 20 m/s. Fig. 3 (a), (c), (e) corresponds to strain of 0.11. The simulations demonstrate the important role of strain localization phenomena in the fracture processes. The calculated plastic strain distributions in the necked zone around the center of the flat sheet sample are presented in Fig. 3(a). Around the center, two shear bands are formed. Fig. 3 (b), (d), (f) showed the configuration of crack. Calculated crack has good agreement with experimental data (see Fig.1 (b)). Good agreement of the location, shape, and length of the cracks with the received in this work experimental data was obtained also at tension velocities 12, 2.4 and 0.4 m/s.

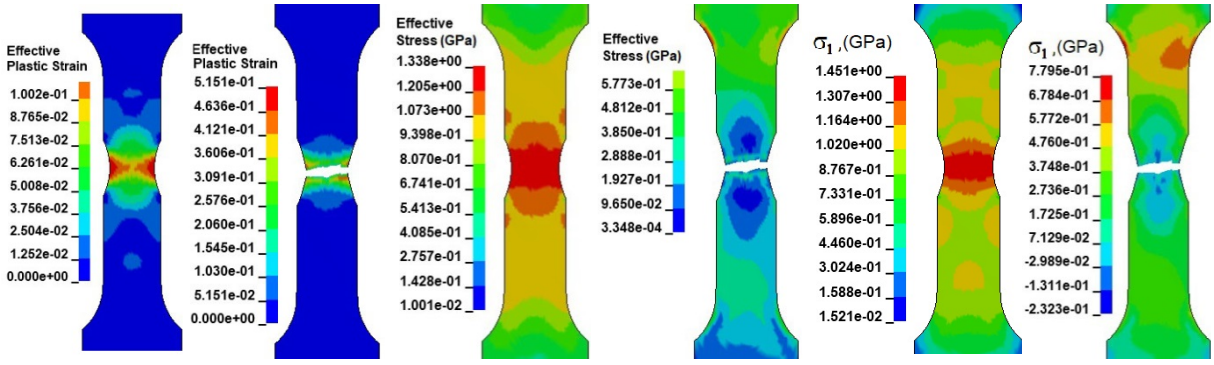


(a) (b) (c) (d) (e) (f)

**Fig. 3.** (a), (b) Calculated effective plastic strain, (c), (d) effective stress, and (e), (f) $\sigma_1$ tensile stress under axial tension at the velocity ~20 m/s

The simulation results in Fig. 4 demonstrate that changes in stress triaxiality in the necking zone have a significant influence on the plastic flow stress and evolution of damage in the alpha titanium alloys at high strain rates.

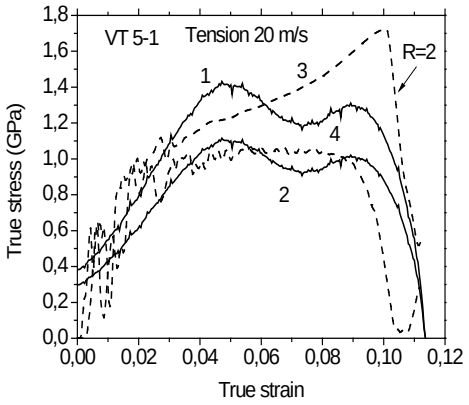


**Fig. 4.** Analytical (curves (1), and (2)) and numerically calculated (curves (3), and (4)) true strain versus true stress in notch sample (R=2 mm) at the velocity of tension 20 m/s. Curves (1), and (3) correspond to notch zone. Curves (2) and (4) correspond to smooth zone of samples

Therefore, the true stress obtained from analytical relations (5) is underestimated relative to the values obtained by numerical simulation. The introduction of the stress triaxiality in the plastic flow model is important for prediction of damage evolution under deformation especially at high strain rates. Damage kinetics in alpha titanium alloys is connected with macroscale plastic instability. This paper presents the experimental and theoretical results demonstrate the importance of an adequate description of the processes of the instability of deformation in titanium alloys.

## Conclusions

This paper has attempted to investigate the mechanical behavior of VT 5-1 (Ti-5Al-2,25Sn) alloy under tension at various strain rates, stress triaxiality, and room temperature. Analysis of the experimental results is supported by FE simulations by which detailed information, complementary to the test results, is obtained on the stress and strain distribution close to the fracture, including the loading path up to the onset of fracture. Significant local plastic strain preceded the formation of a fracture zone in the VT5-1 alloy samples under all the studied loading conditions. In experimental stress-strain curves 1 and 2, shown in Fig. 4, the stage of the formation of macroscopic fracture has a characteristic form for ductile fracture. From the analysis, it is clear that strain localization phenomena play a major role in the fracture process at lower triaxiality. FE simulation in conjunction with appropriate material models, validated by high-quality experiments, is needed to distinguish between material behavior. In this study, the phenomenological strain hardening and damage initiation criterion together with an energy-based law describing the progressive damage evolution were used in the FE models for sheet titanium alloy VT 5-1. The Gurson Tvergaard Needleman plasticity model is adopted for the sheet metal alloy, complemented with phenomenological laws for void nucleation, growth, and coalescence. The FE simulations reproduce the sample dependent competition between a pure, ductile void coalescence fracture and a failure due to macroscopic plastic strain localization.

It is found that the stress triaxiality and strain rate above 10 $s^{-1}$ influence the plastic flow and fracture of alpha titanium alloy. The fracture strain depends noticeably on the stress triaxiality and strain rate too. The constitutive and failure model parameters can be determined based on the tensile test results. The constitutive and fracture models have been validated by simulating the tension tests.

***Acknowledgement.*** *This work was supported by the Russian Science Foundation (RSF), project no. 16-19-10264.*

**References**

[1] Kanel GI, Razorenov SV, Garkushin GV. Rate and temperature dependences of the yield stress of commercial titanium under conditions of shock-wave loading. *Journal of Applied Physics*. 2016;119(18): 185903.

[2] Kanel GI, Garkushin GV, Razorenov SV. Temperature–rate dependences of the flow stress and the resistance to fracture of a VT6 titanium alloy under shock loading at a temperature of 20°C and 600°C. *Technical Physics*. *The Russian Journal of Applied Physics*. 2016;61(8): 1229-1236.

[3] Meshcheryakov YI, Atroshenko SA. On the mesoscopic mechanisms of spall fracture. *Materials Physics and Mechanics.* 2018;36(1): 121-130.

[4] Divakov AK, Mescheryakov YI, Zhigacheva NI, Barakhtin BK, Gooch WA. Spall strength of titanium alloys. *Physical Mesomechanics*. 2010;13(3-4): 113.

[5] Bai Y, Wierzbicki T. A new model of metal plasticity and fracture with pressure and Lode dependence. *International Journal of Plasticity*. 2008;24(6): 1071-1096.

[6] Petrov YV, Kazarinov NA, Evstifeev AD, Bragov AM. Experimental and numerical analysis of the high-speed deformation and erosion damage of the titanium alloy VT-6. *Physics of the Solid State*. 2017;59(1): 93-97.

[7] Volkov IA, Igumnov LA, Ipatov AA, Vorobtsov IV. On the issue of determining parameters in models and criteria of dynamic spallation fracture. *Procedia Engineering.* 2017;197: 244-251.

[8] Volkov IA, Vorobtsov IV, Igumnov LA, Markov IP, Litvinchuk SY. A damaged medium model for describing dynamic spallation fracture. *Procedia Engineering.* 2017;197: 252-259.

[9] Kolobov YR, Perevensentcev VN, Manokhin SS, Kudymova YF, Kolobova AY, Bragov AM, Konstantinov AY. Features of structure formation and development of plastic deformation under dynamic loading of coarse-grained and nanostructured titanium. *Composites and nanostructures*. 2018;8(1): 16-28.

[10] Bobbili R, Madhu V. Effect of strain rate and stress triaxiality on tensile behavior of Titanium alloy Ti-10-2-3 at elevated temperatures. *Materials Science and Engineering A.* 2016;667: 33-41.

[11] Bragov AM, Balandin VV, Konstantinov AY, Lomunov AK, Vorobtsov IV, Kuznetsov AV, Savenkov GG. High-rate deformation and spall fracture of some metals. *Procedia Engineering.* 2017;197: 260-269.

[12] Herzig N, Meyer LW, Musch D, Halle T, Skripnyak VA, Skripnyak EG, Razorenov SV, Krüger L. The mechanical behaviour of ultrafine grained titanium alloys at high strain rates. In: *3rd International Conference on High Speed Forming. March 11-12, 2008. Dortmund, Germany.* 2008. p.141-150.

[13] Skripnyak VA, Skripnyak EG. Mechanical behaviour of nanostructured and ultrafine-grained metal alloy under intensive dynamic loading, Chapter 2: Nanotechnology and Nanomaterials. In: Vakhrushev A. (ed.) *Nanomechanics.* IntechOpen; 2017. p.31-67.

[14] Valoppi B, Brusch S, Ghiotti A, Shivpuri R. Johnson-Cook based criterion incorporating stress triaxiality and deviatoric effect for predicting elevated temperature ductility of titanium alloy sheets. *International Journal of Mechanical Sciences*. 2017;123: 94-105.

[15] Johnson GR, Cook WH. Fracture characteristics of three metals subjected to various strains, strain rates, temperatures and pressures. *Engineering Fracture Mechanics*. 1985;21(1): 31-48.

[16] Marino B, Mudry F, Pineau A. Experimental study of cavity growth in ductile rupture. *Engineering Fracture Mechanics*. 1985;22(6): 989-996.

**[**17] Neilsen KL, Tvergaard V. Ductile shear failure or plug failure of spot welds modelled by modified Gurson model. *Engineering Fracture Mechanics*. 2010;77(7): 1031-1047.
[18] Tvergaard V. Behavior of porous ductile solids at low stress triaxiality in different modes of deformation. *International Journal of Solids and. Structures*. 2015;60-61: 28-34.
[19] Selini N, Elmeguenni M, Benguediab M. Effect of the triaxiality in plane stress conditions. *Engineering, Technology and Applied Science Research*. 2013;3(1): 373-380.